Table S1: Composition of SL by liquid chromatography. The weight percentages were calculated by the signal of oleic acid

component	weight percentage
C16:0	14.6%
C18:2	30.1%
C18:1-FS	42.5%
C18:0	1.1%
C18:1 1x acetate	7.8%
C18:1 2x acetate	0.4%
C18:2 2x acetate	3.1%
C18:1 2x acetate	0.5%

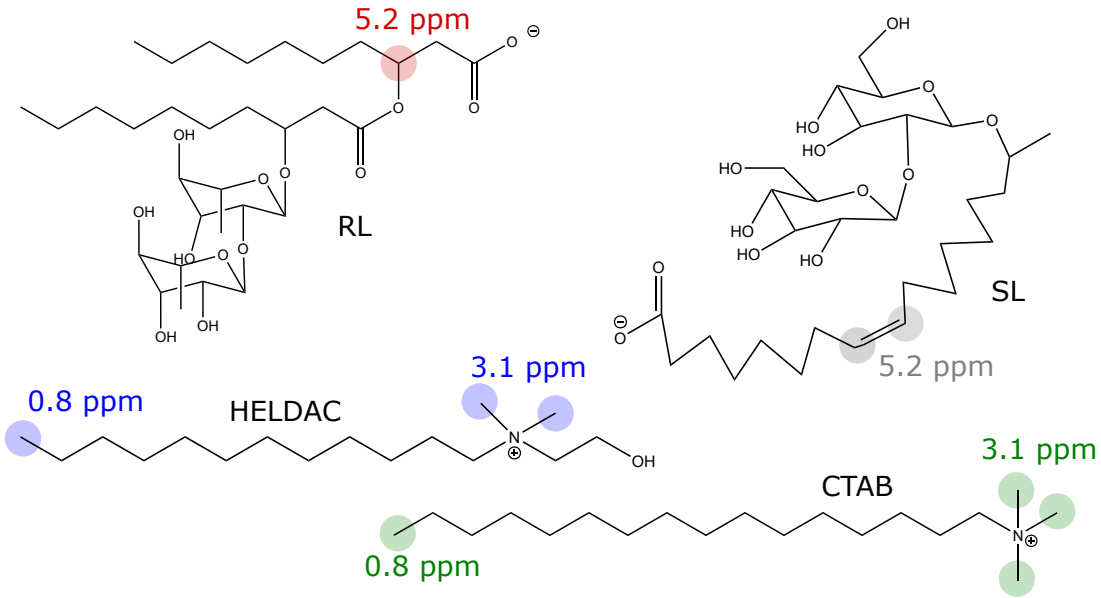

Figure S1: Illustration of the chemical shifts of the studied molecules

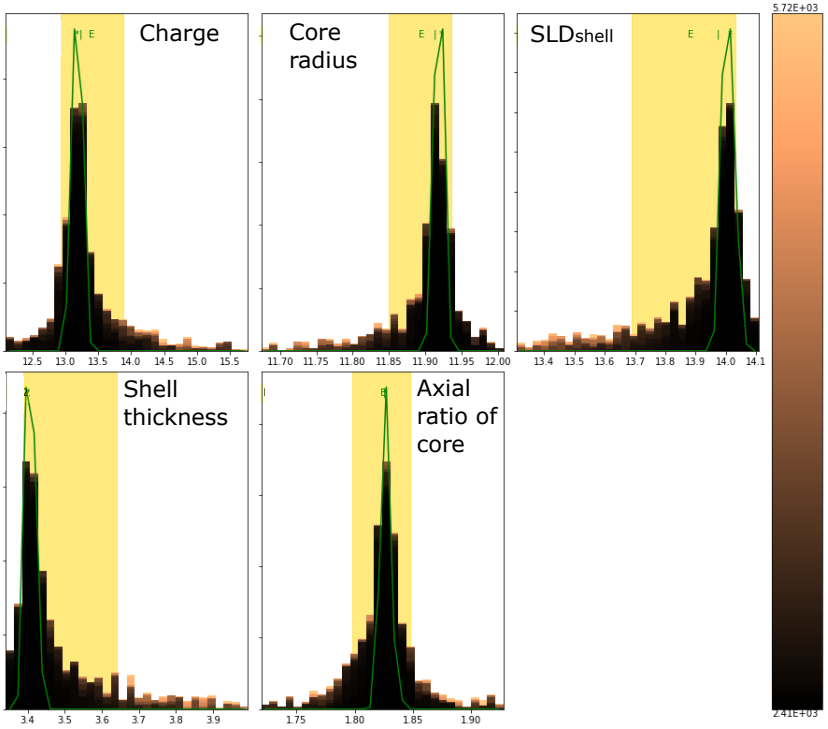

Figure S2: Histograms of the fit parameters resulting from fitting the 100% RL SAXS data with the DREAM algorithm

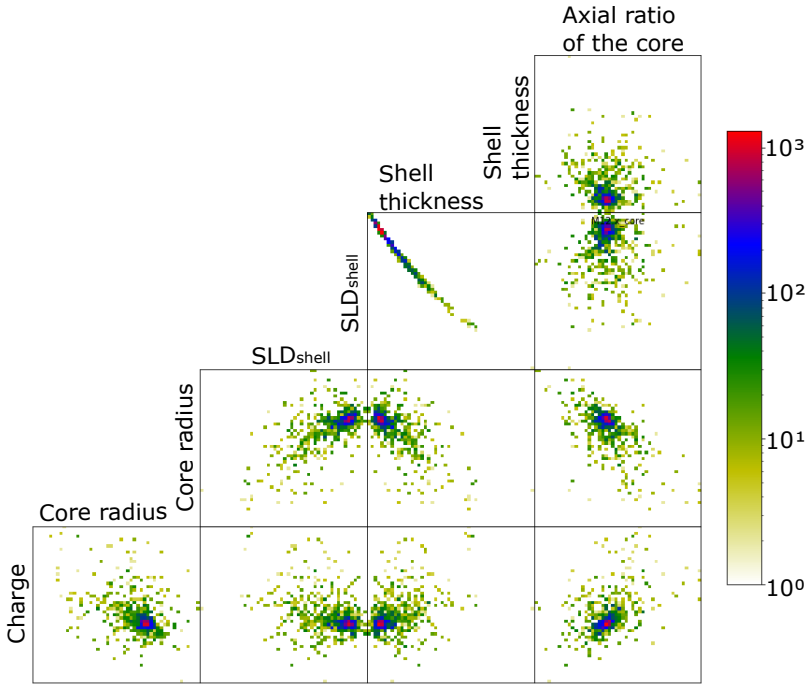

Figure S3: Correlation plots of the fit parameters resulting from fitting the 100% RL SAXS data with the DREAM algorithm

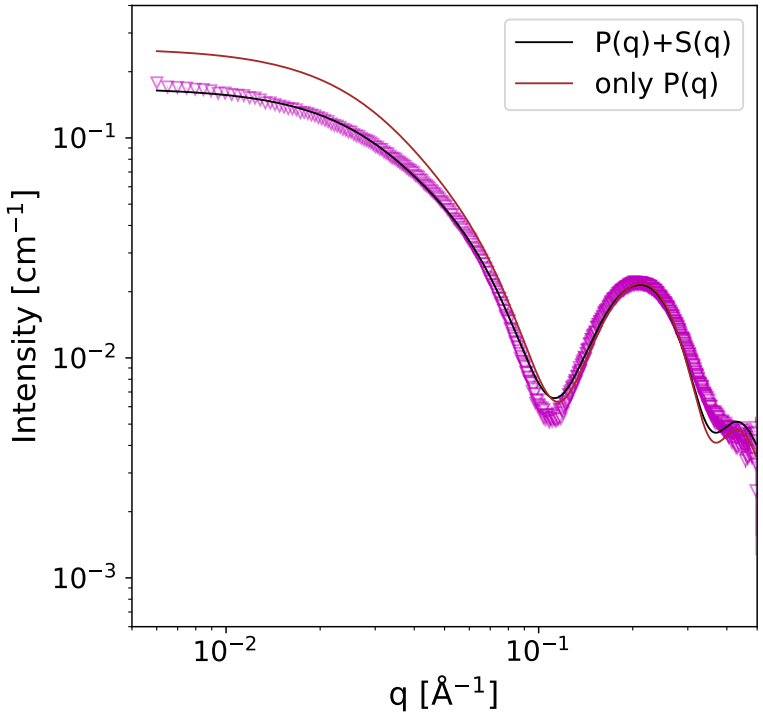

Figure S4: Comparison of fits of the sample 65% RL & 35% HELDAC using the structure factor $S(q)$ (HSA) and form factor $P(q)$ and only $P(q)$

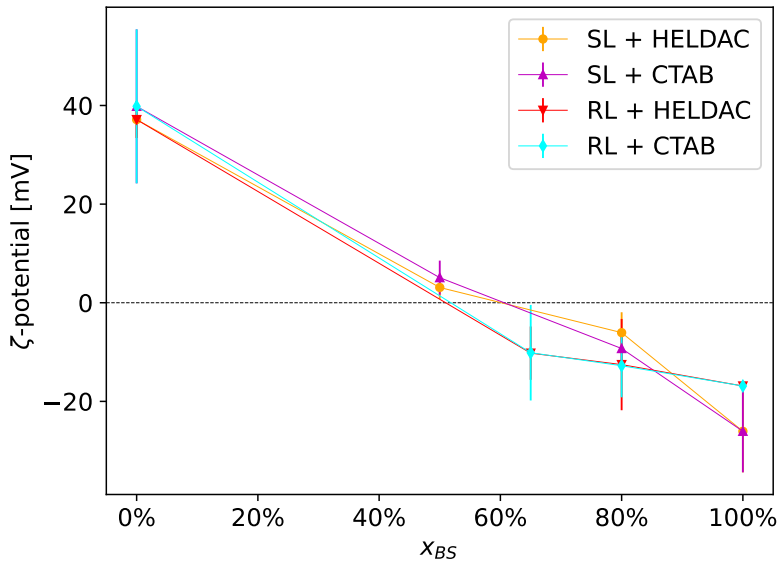

Figure S5: Zeta-potential ζ measurements of the catanionic systems as a function of the fraction of the BSs RL and SL in solution x_{BS} at 20 mM measured by the Litesizer from Anton Paar Germany GmbH. The error bar describes the standard deviation of at least five measurements

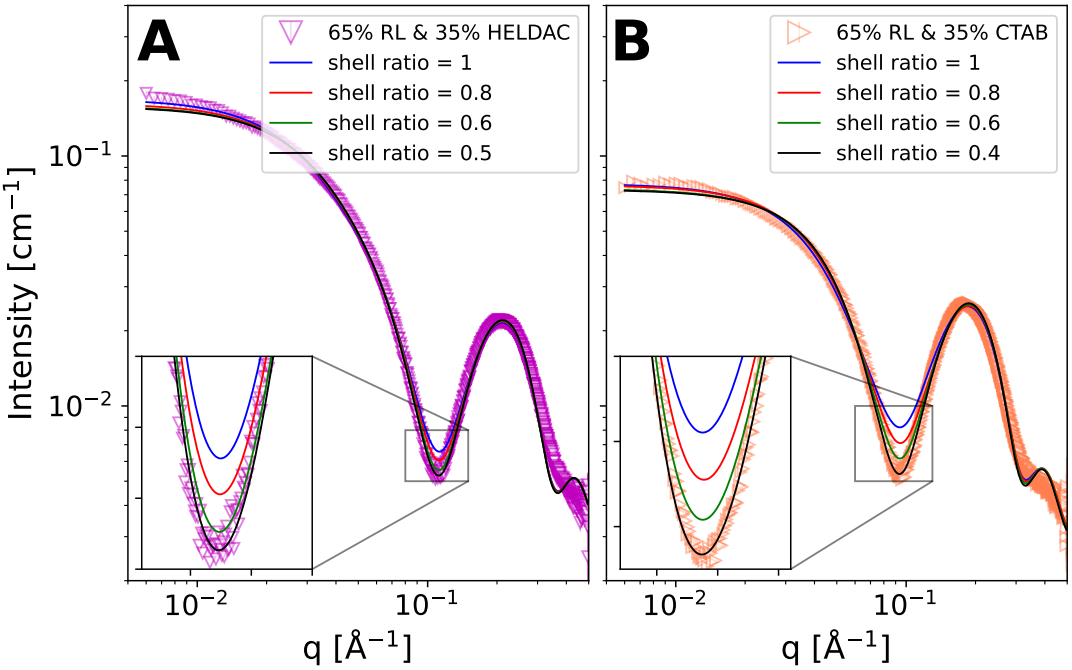

Figure S6: SAXS data of Figure 4 fitted with the HSA + core-shell ellipsoid model assuming different shell ratios. The shell ratios correspond to different thicknesses of the hydrophilic headgroups within the aggregate

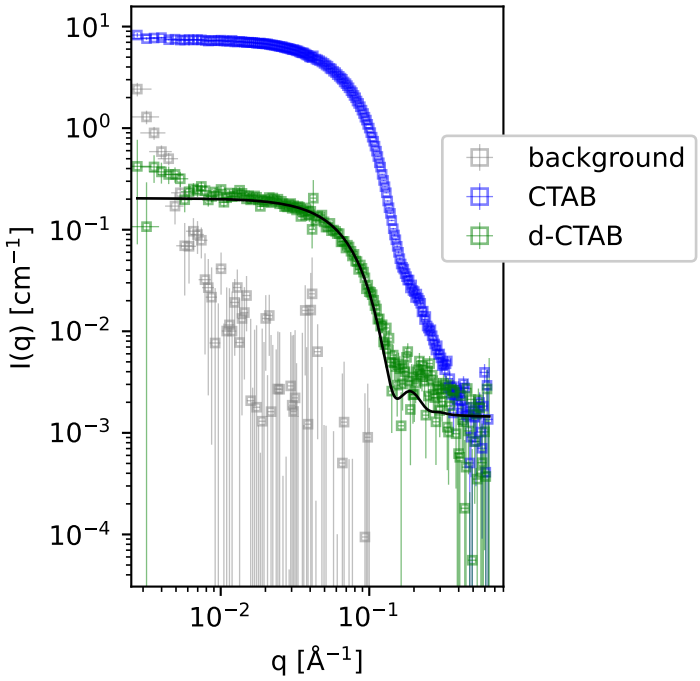

Figure S7: Small-angle neutron scattering of CTAB (blue), deuterated CTAB in contrast matched solvent (green, SLD = $5.86{\cdot}10^{-6}$/Å^2) and buffer (grey, SLD = $5.86{\cdot}10^{-6}$/Å^2). The fit shows a sphere model with the spheres having a radius of 29 Å and SLD of $6.9{\cdot}10^{-6}$/Å^2 while the solvent has a SLD of $5.86{\cdot}10^{-6}$/Å^2

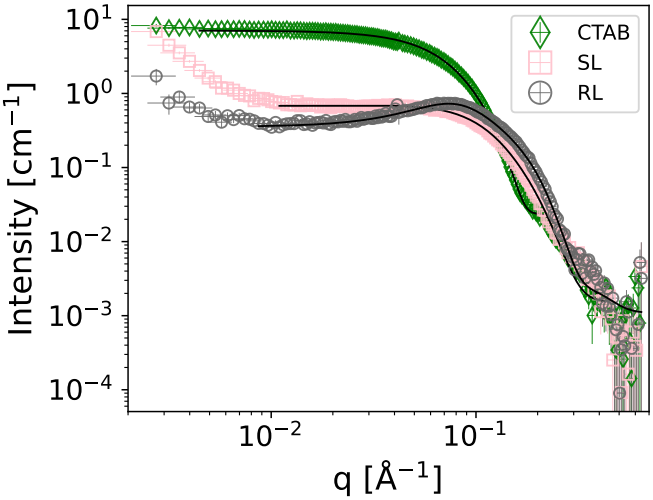

Figure S8: Measured SANS profiles (symbols) and fits (solid lines) of the pure substances CTAB, RL and SL using models of HSA + core-shell ellipsoids

S1 Calculation of the Invariant

It is possible to determine the internal composition of the micelles by calculating the invariants of the curves obtained from comparing the total scattering of the samples with h-CTAB and d-CTAB [1]. Matching the SLD of CTAB and water with d-CTAB, only the biosurfactants remain visible for neutrons and less neutrons are scattered compared to the sample of h-CTAB and RL in which the neutrons get scattered on RL and CTAB molecules. The invariants with d-CTAB, however, have to be corrected because d-CTAB and D_2O did not match completely. Hence, the invariant of d-CTAB in D_2O in Figure S7 (adjusted by the actual used amount of d-CTAB used) was subtracted from those of the mixtures of biosurfactants and d-CTAB. For clarity, here is an example: the invariant of d-CTAB in D_2O in Figure S7 is $6.01{\cdot}10^{-6}/\text{Å}^2$ and the one of 65% RL and 35% d-CTAB in Figure 5 A $5.91{\cdot}10^{-6}/\text{Å}^2$. The d-CTAB content of the d-CTAB in D_2O is 1.64v% and of 65% RL and 35% d-CTAB in D_2O is 0.57v%. The corrected invariant of 65% RL and 35% d-CTAB is then $5.91 \cdot 10^{-4} - 6.01 \cdot 10^{-5} \cdot \frac{0.57}{1.64} = 5.70 \cdot 10^{-6}/\text{Å}^2$). The invariants of the different contrasts can then be correlated with a factor $f = \frac{\text{Invariant}_{\text{bulk}}}{\text{Invariant}_{\text{film}}}$. In the case of our example, it is $f = \frac{1.33}{5.70} = 2.33$. This factor also correlates the differences in SLDs (dSLDs) of the contrasts $f = \frac{\text{dSLD}_{\text{bulk}}{}^2}{\text{dSLD}_{\text{film}}{}^2}$. Therefore, the expected dSLD of the film contrast with d-CTAB can be calculated: $\text{dSLD}_{\text{film}} = \frac{1}{\sqrt{f}} \cdot \text{dSLD}_{\text{bulk}} = \frac{1}{\sqrt{2.33}} \cdot 5.56 \cdot 10^{-6}/\text{Å}^2 = 3.64 \cdot 10^{-6}/\text{Å}^2$. By knowing the differences in the dSLDs of the pure components in water, the composition can be obtained. Here, 73% RL with a dSLD of $5.24 \cdot 10^{-6}/\text{Å}^2$ and 27% CTAB with $-0.63 \cdot 10^{-6}/\text{Å}^2$ equals the expected dSLD of $3.64{\cdot}10^{-6}/\text{Å}^2$.

Strey et al. assumed a total error of 2% for the volume fraction of each substance [1]. However, this estimation represents an ideal case with optimal contrast conditions and an extended q-range. In the present work, additional uncertainties arise from incomplete contrast matching as well as the limited experimental q-range, which may affect the accuracy of the invariant determination. Therefore, the actual uncertainty in the derived composition is expected to be higher.

References

[1] R Strey and M Jonströmer. Role of medium-chain alcohols in interfacial films of nonionic microemulsions. *The Journal of Physical Chemistry*, 96(11):4537–4542, 1992.